Effect of Through-Bond Interaction on Conformation and Structure in Rod-Shaped Donor–Acceptor Systems

Part 1

Crystal Structures of Five *N*-Arylpiperidin-4-one Derivatives

by **Dirk J. A. De Ridder***, **Kees Goubitz**, and **Henk Schenk**

Laboratory for Crystallography, Institute of Molecular Chemistry, Faculty of Science, University of Amsterdam, Nieuwe Achtergracht 166, NL-1018 WV Amsterdam
(phone: (31)-20-525 7039; fax: (31)-20-525 6940; e-mail: dirkdr@science.uva.nl)

and **Bert Krijnen**[1]) and **Jan W. Verhoeven**

Laboratory of Organic Chemistry, Institute of Molecular Chemistry, Faculty of Science, University of Amsterdam, Nieuwe Achtergracht 129, NL-1018 WS Amsterdam

The crystal structures of five *N*-arylpiperidin-4-one derivatives **2P2**, **3P2**, **5P2**, **1P3**, and **2P3** are presented (*Fig. 2* and *Tables 1–5*) and discussed together with the derivatives **1P2** and **4P2** published previously. In all but one structure, **1P2**, the aryl group is in an equatorial position. The piperidine ring adopts a normal chair conformation. In **1P2**, the piperidine ring central C–C bonds are significantly elongated, which is consistent with the idea that through-bond interaction is more pronounced in the axial conformation. Through-bond interaction also influences the pyramidalization at the piperidine C(4)-atom in such a way that a strong interaction is directing the ethylene C-atom C(9) into the axial direction.

1. Introduction. – In 1968, *Hoffmann et al.* [1] introduced the term 'through-bond interaction' (TBI) to designate the intramolecular interaction between functional groups *via* the connecting σ-bonds. According to this concept, the orbitals of the functional groups may interact with each other as a consequence of their mutual mixing with the intervening σ-bonds.

The study of TBI in rod-shaped bichromophoric compounds containing a one-electron donor and acceptor has been a main topic in the research group of *Verhoeven* and co-workers [2–6]. *Krijnen* [7] investigated systematically whether through-bond donor–acceptor interaction can be found in the rod-shaped donor–acceptor compounds shown in *Fig. 1*. Both of these systems contain a substituted N-atom as the potential one-electron donor and a substituted exocyclic C=C bond as the potential acceptor, whereas donor and acceptor are separated by three σ-bonds in a well-defined arrangement. Variations in the *N*-aryl group serve to modify the electron-donating ability of the N-atom, whereas the R substituent will influence the electron affinity of the acceptor.

---

[1]) Permanent address: *Unilever R&D Vlaardingen*, Olivier van Noortlaan 120, 3133 AT Vlaardingen, Netherlands

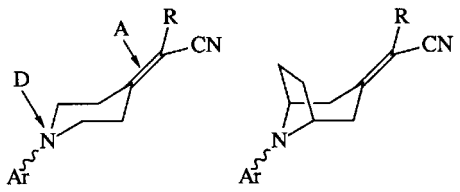

Fig. 1. *Donor–acceptor compounds investigated. Left:* piperidin-4-one-like systems (this paper); *right:* tropan-3-one-like systems [9]. D = Donor, A = Acceptor; R = CN, MeOCO; Ar = Ph, 4-Me–C_6H_4, 3,5-Me_2–C_6H_3, 4-MeO–C_6H_4, 4-F–C_6H_4, 2,4,6-Me_3–C_6H_2.

In the first part of this series of three papers, the crystal structures of five *N*-arylpiperidin-4-one derivatives are presented and discussed together with two *N*-arylpiperidin-4-one derivatives already published [8]. In the second part of this series, the crystal structures of some *N*-aryltropan-3-one derivatives will be discussed [9]. In the crystal structures described in the first two papers, the exocyclic C=C bond carries two CN groups, and one CN and one $COOCH_3$ group, respectively. In the last paper of this series, three *N*-arylpiperidin-4-one derivatives carrying only one non-H substituent on the exocyclic C=C bond, and two piperazine derivatives will be presented [10].

2. Results and Discussion. – The systematic code introduced by *Krijnen* [7] to indicate the compounds studied will also be used here. Piperidine-like systems will be designated by **nPm**, whereas tropane-like systems will be denoted by **nTm** (*cf. Scheme*). The first index **n** indicates which aryl group is attached to the N-atom, whereas the second index **m** codes for the substituent at C(4) of the central piperidine ring. **m** = 0 means that there is no substituent attached to C(4), whereas **m** = 1 means that the CH_2(4) of the piperidine ring is converted to a C(4)=O function. The donor–acceptor systems have been synthesized by *Knoevenagel*-type condensations [11] of the ketones **nP1** and **nT1**. The condensation products of the reaction with malononitrile will be designated by **nP2** and **nT2**, whereas the products of the condensation with methyl cyanoacetate will be denoted as **nP3** and **nT3** (*cf. Scheme*).

X-Ray crystal structures have been determined for the compounds **1P2**–**5P2**, **1P3**, and **2P3**; *Krijnen et al.* [8] already reported the synthesis and X-ray structures of **1P2** and **4P2**. Several attempts to determine the X-ray structure of **6P2** were unsuccessful. Crystallographic data of the new structures are given in *Table 1*, selected bond lengths and angles of all compounds are compiled in *Table 2*. In *Fig. 2*, the ORTEP drawings are presented, showing the atomic-numbering system.

The *N*-aryl group adopts the equatorial position, with the exception of **1P2**, in which the Ph group is found in the axial orientation. From temperature-dependent absorption measurements [7], it has been concluded that, at room temperature in solution, the axial conformation of **1P2** and **3P2** is populated by *ca.* 30% of the molecules, whereas this is decreased in the other **nPm** compounds. The present structures, therefore, give a strong indication that such an axial conformer is thermodynamically feasible under normal conditions.

2.1 *Configuration of the Piperidine Ring.* The strength of TBI is thought to be sensitive to the orientation of the interacting donor and acceptor orbitals with respect

Scheme. *Explanation of the Codes Used to Indicate the Compounds Studied*. At the bottom, the reaction scheme of the *Knoevenagel*-type condensation [11] is shown.

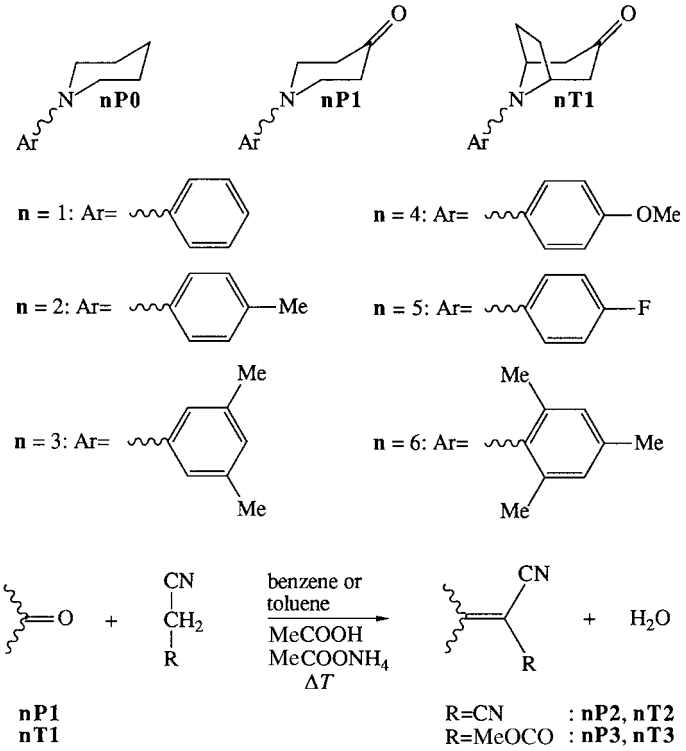

to the σ-relay connecting them, and also for the conformation of the σ-relay itself [1][12]. Consequently, the conformation of the central piperidine ring has to be examined first.

As evident from *Fig. 2*, the piperidine ring in the X-ray structures is found in a chair conformation; least-squares planes have been calculated through C(2)–C(3)–C(5)–C(6) (*a*), C(3)–C(4)–C(5) (*b*), and C(2)–N(1)–C(6) (*c*) to define the ring. The sharp angles between these planes, and the distance of N(1) and C(4) to the central C(2)–C(3)–C(5)–C(6) plane are listed in *Table 3*.

Throughout the **nPm** series, the orientation of the C(2)–C(6) part of the molecule is roughly the same, although a slight flattening is encountered in **1P3**, which has a lower angle between planes *a* and *b*.

In these structures, the orientation of the C(2)–N(1)–C(6) part of the molecule is fairly constant, the angle between *a* and *c* having a small range.

A priori, it has to be expected that, in the **nP2** structures, the piperidine ring displays (near) C_s symmetry, *i.e.*, the bonds N(1)–C(2) and N(1)–C(6), C(3)–C(4) and C(4)–C(5), and C(2)–C(6) and C(5)–C(6), should have (almost) equal lengths. In **3P2**, the piperidine-ring mirror plane coincides with the crystallographic mirror plane, and, therefore, the ring has C_s symmetry. Deviations from this (quasi) C_s symmetry can

Table 1. *Crystallographic Data of* N-*Arylpiperidin-4-ones* **2P2**, **3P2**, **5P2**, **1P3**, *and* **2P3**. For the methods used in the structure determination, see *Exper. Part*. The crystallographic data of **1P2** and **4P2** have been published in [8].

	2P2	**3P2**	**5P2**	**1P3**	**2P3**
Formula	$C_{15}H_{15}N_3$	$C_{16}H_{17}N_3$	$C_{14}H_{12}FN_3$	$C_{15}H_{16}N_2O_2$	$C_{16}H_{18}N_2O_2$
Formula weight	237.3	251.3	241.3	256.3	270.3
Wavelength/Å	0.71069	0.71069	1.5418	0.71069	0.71069
Source	MoK_α	MoK_α	CuK_α	MoK_α	MoK_α
T/K	293	293	293	293	293
a/Å	6.695(1)	13.778(3)	10.6030(7)	14.526(5)	6.621(2)
b/Å	8.078(2)	12.761(2)	15.5439(10)	12.691(3)	11.004(5)
c/Å	12.679(2)	15.687(3)	7.5771(9)	7.246(1)	11.253(3)
α/°	102.59(2)				64.37(2)
β/°	90.81(2)		94.081(9)	104.63(2)	84.44(3)
γ/°	103.22(2)				81.89(3)
V/Å^3	650.0(2)	2758.1(9)	1245.6(2)	1324.6(6)	731.6(5)
Crystal size/mm^3	0.35 × 0.45 × 0.50	0.38 × 0.50 × 0.50	0.20 × 0.30 × 0.45	0.20 × 0.23 × 0.30	0.23 × 0.50 × 0.75
Crystal system	Triclinic	Orthorhombic	Triclinic	Monoclinic	Triclinic
Space group	$P\bar{1}$	*Cmca*	$P2_1/n$	$P2_1/a$	$P\bar{1}$
Z	2	8	4	4	2
D_x/g cm^{-3}	1.21	1.21	1.29	1.29	1.23
μ/mm^{-1}	0.07	0.07	0.73	0.09	0.08
F(000)	252	1072	504	544	288
θ Range/°	1.6 – 34.9	2.5 – 24.8	5.1 – 59.9	2.2 – 30.0	2.0 – 24.9
Measured refls.	5659	1263	1840	3855	2547
Obs. refls ($I > 2.5\sigma(I)$)	1955	976	1588	1263	1719
Refined parameters	164	95	164	173	182
G	3845(156)	30534(1063)	10483(341)	415(67)	5033(207)
R[a])	0.064	0.055	0.053	0.041	0.055
R_w[b])	0.055	0.052	0.060	0.038	0.050
A, B, C[c])	0.22, 0.01, 0.01	2.0, 0.01, 0.01	0.5,0.01,0.01	0.5, 0.01, 0.01	0.25,0.01,0.01
Goodness-of-fit	0.93	1.09	1.03	1.02	1.01
$\Delta\rho$ (max,min)/eÅ^{-3}	0.31, −0.35	0.35, −0.25	0.18, −0.19	0.62, −0.39	0.39, −0.22
CCDC Deposition No.	190407	190408	190409	190410	190411

[a]) $R = \Sigma(|F_{obs}| - k|F_{calc}|)/\Sigma(|F_{obs}|)$. [b]) $R_w = \Sigma w((|F_{obs}| - k|F_{calc}|)^2)/\Sigma(|F_{obs}|^2)$. [c]) $w^{-1} = (A + B \cdot (\sigma(F_{obs}))^2 + C/(\sigma(F_{obs})))$

Table 2. *Selected Bond Lengths* [Å] *and Angles* [°] *with Estimated Standard Deviations in Parentheses.* Σ is the sum of the bond angles at N(1). Data for **1P2** and **4P2** are taken from [8]. For **3P2**, a value in italics indicates that it is equal to that on the line above by symmetry.

	1P2	**2P2**	**3P2**	**4P2**	**5P2**	**1P3**	**2P3**
N(1)–C(2)	1.459(2)	1.465(4)	1.466(3)	1.461(2)	1.454(4)	1.456(4)	1.475(4)
N(1)–C(6)	1.461(2)	1.461(3)	*1.466(3)*	1.459(2)	1.450(4)	1.471(4)	1.468(4)
N(1)–C(10)	1.412(2)	1.429(4)	1.422(5)	1.423(2)	1.412(4)	1.402(4)	1.426(4)
C(2)–C(3)	1.546(2)	1.524(4)	1.538(4)	1.526(2)	1.525(5)	1.512(5)	1.487(5)
C(5)–C(6)	1.542(2)	1.526(4)	*1.538(4)*	1.529(2)	1.522(5)	1.521(5)	1.511(4)
C(3)–C(4)	1.494(2)	1.487(4)	1.487(3)	1.489(2)	1.490(5)	1.510(4)	1.512(5)
C(4)–C(5)	1.495(2)	1.491(4)	*1.487(3)*	1.489(2)	1.481(5)	1.504(4)	1.507(4)
C(2)–N(1)–C(6)	109.9(2)	111.1(2)	112.6(2)	111.3(1)	112.1(3)	110.5(3)	109.6(3)
C(2)–N(1)–C(10)	118.9(2)	116.3(2)	117.9(2)	115.9(1)	116.9(3)	120.3(2)	111.6(2)
C(6)–N(1)–C(10)	118.6(2)	116.5(2)	*117.9(2)*	116.4(1)	117.1(3)	120.6(3)	115.8(2)
Σ	347.4(3)	343.9(3)	348.4(3)	343.6(2)	346.1(5)	351.4(5)	337.0(4)

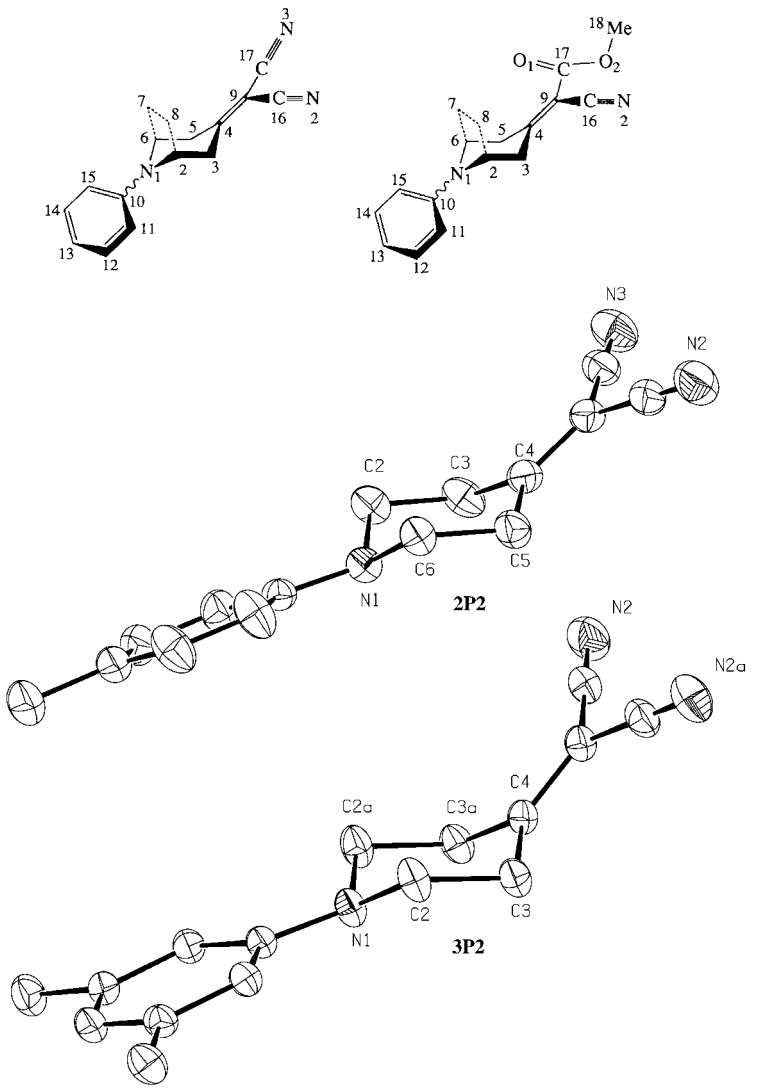

Fig. 2. *Atomic numbering* (arbitrary) *scheme in* **nPm**. *ORTEP* [20] *drawings of* **2P2**, **3P2**, **5P2**, **1P3**, *and* **2P3**. The shapes of the ellipsoids correspond to 30% probability contours of atomic displacement. The H-atoms have been omitted for clarity.

occur when the aryl group is strongly twisted around the N(1)–aryl bond, by an asymmetry in the acceptor part of the molecule (*e.g.*, in the structures **nP3** containing an asymmetrically substituted exocyclic C=C bond), or by distortions of the solid state structure due to crystal packing effects. The asymmetry parameters (*Table 3*) introduced by *Duax et al.* [13] indicate that the deviations from (quasi) C_s symmetry are very small, indicating that the piperidine ring adopts a normal chair conformation.

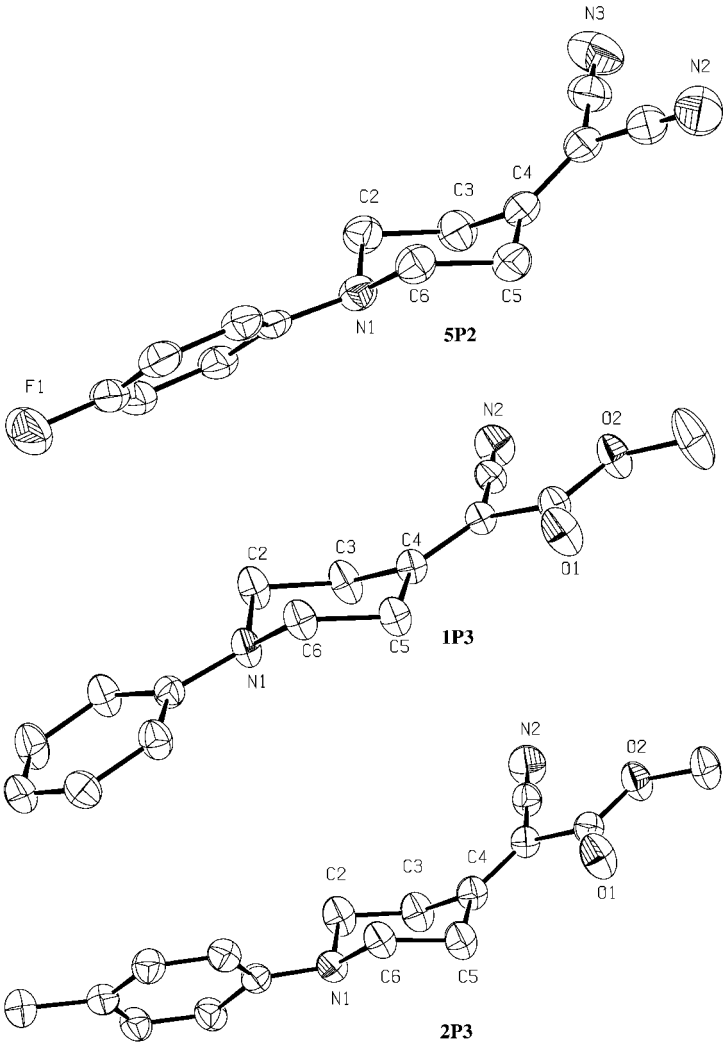

Fig. 2. (cont.)

Because of crystallographic symmetry in **3P2**, the asymmetry parameter is equal to zero.

The bond lengths (*Table 2*) indicate that the piperidine ring in **5P2** is not symmetric, which can be related to the pronounced twist of the aryl group around the N(1)–aryl bond (see *Sect. 2.2*), which induces an asymmetry in the molecule. The piperidine ring in the other **nP2** structures is highly symmetric. In the structures containing the asymmetric acceptor chromophore (**1P3** and **2P3**), the piperidine ring is asymmetric in all cases (*Table 2*), especially regarding the central C(2)–C(3) and C(6)–C(5) bonds.

2.2 *Configuration at the Piperidine N-Atom.* In all compounds, the piperidine N-atom N(1) adopts a flattened pyramidal configuration, as indicated by the sum of the

Table 3. *Angles* [°] *between Calculated Least-Squares Planes and Distances* [Å] *of N(1) and C(4) to the Central Plane* a *Defined by C(2), C(3), C(5), and C(6); Plane* b *Defined by C(3), C(4), and C(5); Plane* c *Defined by C(2), N(1), and C(6)*. Data for **1P2** and **4P2** are taken from [8]; e.s.d.'s calculated with XTAL3.7 [18] from CIF. Asymmetry parameter ΔC_s calculated according to *Duax et al.* [13].

	1P2	**2P2**	**3P2**	**4P2**	**5P2**	**1P3**	**2P3**
Angle between planes *a* and *b*	49.0(2)	41.9(3)	50.0(3)	42.0(2)	44.3(3)	36.7(3)	44.2(3)
Angle between planes *a* and *c*	55.1(2)	53.2(3)	51.9(3)	53.9(2)	53.8(3)	54.7(3)	53.6(3)
Distance of N(1) to plane *a*	−0.687(3)	−0.663(3)	−0.641(4)	−0.666(3)	−0.654(4)	−0.680(4)	−0.684(4)
Distance of C(4) to plane *a*	0.614(3)	0.537(4)	0.629(4)	0.538(3)	0.559(5)	0.492(5)	0.578(5)
ΔC_s	1.4	0.5	0	2.0	0.8	0.5	3.2

bond angles at N(1) (Σ in *Table 2*). This sum is fairly constant (343.6(2)–351.4(5)°), with the exception of **2P3** in which the significantly smaller angles C(2)–N(1)–C(10) and C(6)–N(1)–C(10) result in a smaller sum of the bond angles at N(1) (337.0(4)°). AM1 Calculations performed on the *N*-arylpiperidines **nP0** predicted this sum to be *ca.* 345° [7], which is thus in good agreement with (most of) the aforementioned values.

From the torsion angles along the N(1)–C(10) bond, the orientation of the aryl group can be derived (*Table 4*). When the N-atom lone pair and the aromatic π-system are completely aligned, the torsion angles C(2)–N(1)–C(10)–C(11) (τ_1) and C(6)–N(1)–C(10)–C(15) (τ_2) should be (almost) equal. The twist angle β, *i.e.*, the deviation from complete alignment of the lone pair and the π-system, can be calculated as $\beta = ½\,||\,\tau_1\,| - |\,\tau_2\,||$ (see *Table 4*).

Table 4. *Absolute Values of Selected Torsion Angles* [°] *along the N(1)–C(10) Bond and Calculated Values of the Twist Angles β*. Data for **1P2** and **4P2** are taken from [8]; e.s.d.'s calculated with XTAL3.7 [18] from CIF. For **3P2**, $\tau_1 = \tau_2$ by symmetry.

	1P2	**2P2**	**3P2**	**4P2**	**5P2**	**1P3**	**2P3**
C(2)–N(1)–C(10)–C(11) (τ_1)	21.8(3)	36.0(4)	22.2(5)	45.3(2)	49.7(4)	14.2(5)	63.3(5)
C(6)–N(1)–C(10)–C(15) (τ_2)	22.7(4)	14.4(5)	*22.2(5)*	4.7(3)	4.4(4)	25.1(5)	10.7(5)
$\beta = ½\,\|\,\tau_1\,| - |\,\tau_2\,\|$	0.5(3)	10.8(3)	0	20.3(2)	22.7(3)	5.5(4)	26.3(4)

From both experiments and calculations [7], it has been concluded that in *N*-arylpiperidines $\beta = 30–50°$, independent of the conformation, *i.e.*, axial or equatorial orientation of the aryl group. Furthermore, AM1 calculations [7] performed on the equatorial and axial conformation of **1P2** predict $\beta \approx 24°$ for both conformers. In the axial X-ray structure **1P2**, however, this twist angle is only 0.5(3)°.

In the equatorial X-ray structures, the spread in the angle β ($0° < \beta < 26.3(4)°$) is great, indicative for a less pronounced preference for alignment of the N-atom lone pair and the aromatic π-system than in the axial X-ray structure. The values of β for **5P2** and **2P3** are, in fact, very close to those predicted by the AM1 calculations performed on **nP0** [7]. It seems, therefore, that the twist angle β in the X-ray structures of the donor–acceptor systems depends on the equatorial or axial orientation of the aryl group, which

is in contrast with the predictions of the AM1 calculations performed on related systems, although it should be noted that these latter results refer to the gas phase and not to the solid state.

In general, a larger twist angle β is coupled to a small value of the sum of the bond angles Σ at N(1) (*Table 2*). In **2P3**, Σ is minimal (337.0(4)°) and β is maximal (26.3(4)°), whereas, in the structures with a very small β, the sum is large (343.9(3)–351.4(5)°); the correlation coefficient between Σ and β is -0.75. There is also a negative correlation between Σ and bond length N(1)–C(10) (-0.73). It seems, therefore, plausible that the observed flattening of N(1) is related to conjugative interaction within the anilino chromophore, and, consequently, this flattening must be related to the twist angle β and bond length N(1)–C(10). From the present data, however, no conclusion can be drawn whether the strength of this conjugative interaction depends on the type, position, and number of substituents on the phenyl ring.

In the equatorial compounds **2P2**, **3P2**, and **1P3**, there are quite short intramolecular H···H contacts (< 1.9 Å) between the piperidine and phenyl ring H-atoms. This correlates with the small β angles for these compounds. Apparently, the interaction between the N-atom lone pair and the aromatic π-system overrides the steric strain caused by the intramolecular H···H contacts. Probably, this is not the case in the other compounds because of crystal-packing effects.

2.3 *Elongation of the 'Central' C–C Bond under the Influence of TBI.* It has been found, *e.g.*, by *Mislow*, *Dougherty*, and co-workers [14] that, in the solid state, TBI between two functionalities may result in a bond elongation of the central C–C bond in the σ-frame connecting these functionalities. In the **nPm** compounds, TBI could thus manifest itself in an elongation of the C(2)–C(3) and the C(5)–C(6) bonds. In piperidine derivatives, the accepted value of the central C–C bond is 1.52–1.53 Å.

The values found for the equatorial structures **2P2**, **4P2**, and **5P2** (1.522(5)–1.529(2) Å) and **nP3** (1.487(5)–1.521(5) Å) testify the absence of strong TBI in these equatorial structures. It is evident that the axial Ph group in **1P2**, thus allowing optimal TBI, results in a significant bond elongation: the central C–C bond has a mean length of 1.544(1) Å in this structure. Comparing this value to those of **2P2**, **4P2**, and **5P2** reveals that TBI results in a bond elongation of at least 0.01 Å. The mean value (1.538(3) Å) of the central C–C bond in **3P2** is close to the corresponding bond length in **1P2**, which may be indicative to a non-negligible TBI.

2.4 *Pyramidalization at C(4).* To study the pyramidalization at the piperidine ring C(4)-atom the torsion angles along the C(4)–C(9), C(3)–C(4), and C(5)–C(4) bonds were calculated (*Table 5*). The flattening of the C(2)–C(6) part of the molecule noted previously for **1P3** (*cf. Sect. 2.1*) is nicely reflected in a decrease of the torsion angles C(2)–C(3)–C(4)–C(5) and C(6)–C(5)–C(4)–C(3) and an increase of the torsion angles H_{eq}–C(3)–C(4)–C(9) and H_{eq}–C(5)–C(4)–C(9) compared to the other structures.

Substituted alkenes are known to show often slight deviations from planarity [15] if the two alkene C-atoms, and the four attached atoms cannot define a plane of molecular symmetry. Inspection of the torsion angles (*Table 5*) reveals a significant non-coplanarity in the acceptor moiety: in the case of coplanarity C(3)–C(4)–C(9)–C(16) and C(5)–C(4)–C(9)–C(17) should be equal to zero.

Table 5. *Absolute Values of Selected Torsion Angles* [°] *along the C(4)–C(9), C(3)–C(4), and C(5)–C(4) Bonds.* Data for **1P2** and **4P2** are taken from [8]; e.s.d.'s calculated with XTAL3.7 [18] from CIF. For **3P2**, the torsion angles along C(5)–C(4) (in italics) are equal to the equivalent ones along C(3)–C(4) by symmetry.

	1P2	**2P2**	**3P2**	**4P2**	**5P2**	**1P3**	**2P3**
Along C(4)–C(9)							
C(3)–C(4)–C(9)–C(16)	3.5(4)	1.5(5)	1.5(6)	1.3(4)	0.2(5)	3.2(5)	4.3(5)
C(5)–C(4)–C(9)–C(17)	2.0(4)	0.1(5)	1.5(6)	2.9(4)	3.3(5)	0.2(6)	8.0(6)
Along C(3)–C(4)							
C(2)–C(3)–C(4)–C(5)	52.4(3)	46.1(4)	54.6(3)	46.7(3)	48.2(4)	40.8(4)	47.8(5)
H_{eq}–C(3)–C(4)–C(9)	3	13.3(5)	2.8(5)	14	8.8(5)	24.1(5)	11.0(5)
H_{ax}–C(3)–C(4)–C(5) (τ_a)	63	74.0(4)	65.5(3)	70	72.1(4)	79.9(4)	72.2(4)
H_{ax}–C(3)–C(4)–C(9) (τ_b)	119	104.8(4)	116.9(4)	108	109.3(3)	94.6(4)	105.6(4)
$\Sigma_1 = \lvert\tau_a\rvert + \lvert\tau_b\rvert$	182	178.8(6)	182.4(5)	178	181.4(5)	174.5(6)	177.8(6)
Along C(5)–C(4)							
C(6)–C(5)–C(4)–C(3)	53.3(3)	46.0(4)	*54.6(3)*	45.7(3)	48.7(4)	40.7(5)	49.5(5)
H_{eq}–C(5)–C(4)–C(9)	1	13.6(5)	*2.8(5)*	12	8.2(5)	24.5(5)	10.7(6)
H_{ax}–C(5)–C(4)–C(3) (τ_c)	58	75.8(3)	*65.5(3)*	71	72.3(4)	80.0(4)	70.1(4)
H_{ax}–C(5)–C(4)–C(9) (τ_d)	127	102.9(3)	*116.9(4)*	107	109.1(3)	94.2(4)	107.5(4)
$\Sigma_2 = \lvert\tau_c\rvert + \lvert\tau_d\rvert$	185	178.7(4)	182.4(5)	178	181.4(5)	174.2(6)	177.6(6)
$\theta = ½\,(\Sigma_1 + \Sigma_2) - 180°$	3.5	−1.2(4)	2.4(4)	−2	1.4(4)	−5.6(4)	−2.4(4)

There are two types of distortions from the ideal planar geometry: twisting around the C(4)–C(9) bond and pyramidalization at C(4). In, *e.g.*, the structures **4P2** and **2P3**, a slight twist around C(4)–C(9) is found, perhaps as the result of crystal-field effects.

More interesting, however, is the pyramidalization at C(4). *A priori,* this distortion can direct C(9) in two different directions as indicated in *Fig. 3*. The angle θ, defined in *Fig. 3*, is a measure for the degree and direction of the pyramidalization at C(4). A negative value for θ indicates an equatorial bending of C(9) and a positive θ bending into the axial direction.

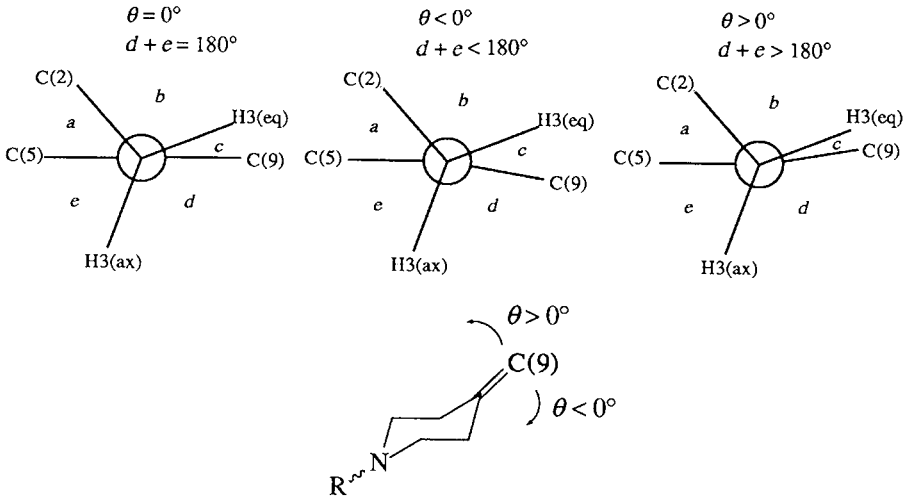

Fig. 3. *Possible modes of pyramidalization at C(4) and the corresponding* Newman *projections along the C(3)–C(4) bond*; $\theta = (d + e) - 180°$.

Theoretical studies on alkenes and carbonyls [15][16] predict that the C-atom will pyramidalize toward a staggered geometry in order to relieve torsional interactions between the allylic bonds and the two σ-bonds and π-orbitals attached to the alkene C-atom. Such a pyramidalization toward the bond most parallel with the π-system is confirmed by a survey of neutron-diffraction crystal structures of amino acids and dipeptides [16]. For our systems, this would correspond to a bending of C(9) into the equatorial direction, thus toward $H_{ax}-C(3)$ and $H_{ax}-C(5)$ (θ negative).

In *Table 5*, the values for θ, obtained by averaging the θ values determined from the torsion angles along the C(3)–C(4) and C(5)–C(4) bonds, are listed.

Pyramidalization into the axial direction ($\theta > 0°$) leads to a greater electron density of the π-orbital on C(4) into the equatorial direction. Consequently, the π-lobe on C(4) becomes more antiparallel to the central C–C bond, thus allowing more effective coupling of the acceptor with the N(1) lone pair. Such donor–acceptor interactions result in an enthalpic stabilization of the molecular system. Therefore, the energetically unfavorable distortion of the C=C bond, *i.e.*, the bending of C(9) resulting in a pyramidalization at C(4) with $\theta > 0°$, is probably compensated by a stabilization offered by an increase of the donor–acceptor interaction upon such a pyramidalization.

If so, a pyramidalization with $\theta > 0°$ has to be anticipated for **1P2** (axial Ph group), whereas, for the other **nPm** structures, a negative pyramidalization is expected, because of the much weaker TBI in structures with an equatorial aryl group. As evident from *Table 5*, the pyramidalization in **1P2** is indeed positive ($\theta = +3.5°$), whereas the structures **2P2**, **4P2**, **1P3**, and **2P3** have negative θ values. Although TBI is maximal in the axial conformation of the donor–acceptor systems, non-negligible TBI also occurs in the equatorial conformation, and this weak TBI might result in a small positive θ as found for **3P2** and **5P2**. The assumption that, especially in the structure **3P2**, some minor manifestations of TBI are encountered, is also supported by the fact that the central C–C bond in this structure (mean value 1.538(3) Å) is somewhat elongated compared to the other structures with an equatorial aryl group (*Table 2*). In the case of **5P2**, however, the central C–C bond shows no elongation (mean value 1.528(4) Å), indicating the absence of TBI. It should be stressed, however, that crystal-packing effects could also result in the small positive θ values observed for **3P2** and **5P2**!

3. Conclusions. – In the available X-ray structures of the **nPm** compounds, the aryl group is found in the equatorial orientation, with the exception of **1P2**, in which an axial preference of the Ph group is found in the solid state. In **1P2**, the central C–C bond is significantly elongated, whereas, in the structures with an equatorial aryl group, such elongation is virtually absent. These observations are consistent with the assumption that in the equatorial conformation TBI is far less pronounced than in the axial conformation.

Not only the central C–C bond is influenced by the donor–acceptor interaction, but also the pyramidalization at C(4). The X-ray structures indicate that, in general, the degree and direction of this pyramidalization is mainly controlled by TBI. In structures with strong TBI – judged from the pronounced elongation of the central C–C bond – the pyramidalization at C(4) directs C(9) into the axial direction. In structures with a less pronounced TBI – equatorial aryl group – this pyramidalization is reduced or directs C(9) into the sterically preferred equatorial direction.

Experimental Part

1. *X-Ray Crystal Structure Determinations.* The reflections were collected on an *Enraf-Nonius CAD-4* diffractometer with graphite monochromated CuK_α or MoK_α radiation (*Table 1*). The unit-cell dimensions resulted from a least-squares fit of the setting angles of 23 centred reflections. The structures were solved by CRUNCH [17] and refined with XTAL3.7 [18]. Full-matrix least-squares refinement was used, anisotropic for non-H-atoms and isotropic for H-atoms. The H-atoms were kept fixed at their calculated positions with fixed $U_{eq} = 0.10$ Å^2. An extinction correction [19] was applied, but no absorption correction.

The crystallographic data (excluding structure factors) of all new structures presented in *Table 1* and *Fig. 2* [20] have been deposited with the *Cambridge Crystallographic Data Centre* (*CCDC*); deposition numbers are given in *Table 1*. Copies of the data can be obtained, free of charge, on application to the *CCDC*, 12 Union Road, Cambridge, CB2 1EZ, UK (fax: +44-1223-336033; e-mail: deposit@ccdc.cam.ac.uk).

2. *Syntheses.* The compounds can be synthesized by *Knoevenagel*-type condensation [11] of malononitrile (for **nP2** compounds) or methyl cyanoacetate (for **nP3** compounds) and the appropriate ketones **nP1** (*Scheme*).

2.1. *Synthesis of* N-*Arylpiperidin-4-ones* **nP1**. 2.1.1. *1-(4-Methylphenyl)piperidin-4-one* (**2P1**). A soln. of 1,5-dichloropentan-3-one (1.00 g, 6.45 mmol) and a soln. of 1.1 equiv. of *p*-toluidine (0.76 g, 7.09 mmol), both in 20 ml of MeOH (dried over mol. sieves 4 Å), were added simultaneously to a stirred slurry of 1.40 g of Na_2CO_3 in 25 ml of dry MeOH during *ca.* 0.75 h. After the addition of the two solns., the mixture was refluxed for 1–1.5 h. After cooling to r.t., 100 ml of Et_2O was added. The mixture was dried ($MgSO_4$), filtered over a fine glass filter, and evaporated to give a light yellow oil. Purification by flash column chromatography (FC) (petroleum ether 40–60/Et_2O 1:1) yielded an almost colorless liquid, which solidified to give **2P1**. White solid. Yield: 0.63 g (3.33 mmol, 47% calculated on *p*-toluidine). M.p. 25–29°. IR ($CHCl_3$): 3000*w*, 2960*s*, 2920*s*, 2810*m*, 1708*s*, 1610*s*, 1510*s*, 810*s*. ^{1}H-NMR (200 MHz, $CDCl_3$): 7.12 (*d*, $J \approx 8.5$, H–C(3), H–C(4) of Ph); 6.91 (*d*, $J \approx$ 8.6, H–C(2), H–C(6) of Ph), 3.55 (*t*, $J \approx 6.0$, CH_2(2), CH_2(6)); 2.55 (*t*, $J \approx 6.0$, CH_2(3), CH_2(5)); 2.29 (*s*, Me).

2.1.2. *1-(3,5-Dimethylphenyl)piperidin-4-one* (**3P1**) was prepared as described for **2P1** by using 3,5-dimethylaniline (0.86 g, 7.10 mmol) instead of *p*-toluidine. The same workup and purification as for **2P1** yielded an almost colorless oil, which solidified to **3P1**. White solid. Yield: 0.71 g (3.49 mmol, 49%). M.p. 40–44°. IR ($CHCl_3$): 3000*w*, 2995*s*, 2960*s*, 2915*s*, 2815*m*, 1705*s*, 1590*s*, 1470*s*, 828*s*. ^{1}H-NMR (200 MHz, $CDCl_3$): 6.62 (*s*, H–C(2), H–C(6) of Ph); 6.57 (*s*, H–C(4) of Ph); 3.59 (*t*, $J \approx 6.0$, CH_2(2), CH_2(6)); 2.55 (*t*, $J \approx 6.0$, CH_2(3), CH_2(5)); 2.30 (*s*, 2 Me).

2.1.3. *1-(4-Fluorophenyl)piperidin-4-one* (**5P1**) was synthesized as described for **2P1** by using 2.8 g of Na_2CO_3 in 50 ml of MeOH, 1,5-dichloropentan-3-one (2.00 g, 12.9 mmol) and 4-fluoroaniline (1.43 g, 12.9 mmol). The mixture was refluxed (1.5 h) and then evaporated to *ca.* 50 ml. After the addition of 150 ml of a 0.1 M KOH soln., the turbid mixture was extracted 3 times with CH_2Cl_2. The combined org. layers were dried ($MgSO_4$), filtered, and evaporated to yield a brown oil. FC (silica gel; petroleum ether 40–60/Et_2O 1:1) yielded the products as an off-white solid. Recrystallization from petroleum ether 40–60/Et_2O yielded **5P1**. Cream-colored solid. Yield: 0.73 g (3.78 mmol, 29%). M.p. 77–79°. IR ($CHCl_3$): 3000*w*, 2995*m*, 2980*m*, 2900*m*, 2800*m*, 1705*s*, 1500*s*, 822*s*, 809*s*. ^{1}H-NMR (200 MHz, $CDCl_3$): 6.97 (*m*, 4 arom. H); 3.50 (*t*, $J \approx 6.1$, CH_2(2), CH_2(6)); 2.57 (*t*, $J \approx 6.1$, CH_2(3), CH_2(5)).

2.2. *Syntheses of the Donor–Acceptor Systems* **nP2** *and* **nP3**. 2.2.1. *2-[1-N(4-Methylphenyl)pyrrolidin-4-ylidene]propanedinitrile* (**2P2**) was synthesized by stirring and refluxing the ketone **2P1** (0.21 g, 1.11 mmol), malononitrile (83 mg, 1.26 mmol), 120 mg of $AcONH_4$, and 0.20 ml of AcOH in 10 ml of toluene for 1 h in a *Dean-Stark* apparatus. After cooling, some toluene was added (*ca.* 20 ml), and the same workup as for **1P2** [8] yielded a dark brown residue. FC (silica gel; petroleum ether 40–60/Et_2O 3:2) yielded 0.15 g of a yellow solid. Recrystallization from cyclohexane/Et_2O (with a few drops of CH_2Cl_2) yielded **2P2**. Large yellow crystals, suitable for X-ray analysis. Yield: 0.15 g (0.63 mmol, 57%). M.p. *ca.* 111° (dec.). IR ($CHCl_3$): 3020*m*, 2995*m*, 2955*m*, 2910*m*, 2805*m*, 2210*s*, 1590*s*, 1505*s*, 804*s*. ^{1}H-NMR (200 MHz, $CDCl_3$): 7.12 (*d*, $J \approx 8.3$, H–C(3), H–C(5) of Ar); 6.87 (*d*, $J \approx 8.6$, H–C(2), H–C(6) of Ar); 3.45 (*t*, $J \approx 5.6$, CH_2(2), CH_2(6)); 2.86 (*t*, $J \approx 5.6$, CH_2(3), CH_2(5)); 2.29 (*s*, Me). ^{13}C-NMR (50.3 MHz, APT, $CDCl_3$): 180.6 (C(4)). 146.3 (C(1) of Ar); 130.3 (C(4) of Ar); 130.0 (C(3), C(5) of Ar); 116.5 (C(2), C(5) of Ar); 111.3 (CN); 83.4 (C(4)=*C*); 50.3 (C(2), C(6)); 33.5 (C(3), C(5)); 20.3 (Me). HR-MS: 237.1280 ($C_{15}H_{15}N_3^+$; calc. 237.1266).

2.2.2. *2-[1-(3,5-Dimethylphenyl)pyrrolidin-4-ylidene]propanedinitrile* (**3P2**) was synthesized by refluxing **3P1** (0.25 g, 1.23 mmol), malononitrile (95 mg, 1.44 mmol), 95 mg of $AcONH_4$, and 0.22 ml of AcOH in 10 ml of toluene for 1 h in a *Dean-Stark* apparatus. After the same workup as for **2P2**, the product was purified by FC (silical gel; petroleum ether 40–60/Et_2O 1:1) and subsequent recrystallization from Et_2O/CH_2Cl_2 1:1 yielded **3P2**. Light-yellow crystals. Yield: 0.20 g (0.80 mmol, 65%). M.p. *ca.* 150° (dec.). IR ($CHCl_3$): 3030*w*, 3000*m*,

2960*m*, 2920*m*, 2820*m*, 2225*s*, 1590*s*, 825*m*. ^{1}H-NMR (200 MHz, $CDCl_3$): 6.59 (*s*, 3 arom. H); 3.48 (*t*, $J \approx 5.6$, $CH_2(2)$, $CH_2(6)$); 2.84 (*t*, $J \approx 5.6$, $CH_2(3)$, $CH_2(5)$); 2.30 (*s*, 2 Me). ^{13}C-NMR (62.9 MHz, APT, $CDCl_3$): 180.7 (C(4)); 148.5 (C(1) of Ar); 139.2 (C(2), C(5) of Ar); 122.6 (C(4) of Ar); 114.1 (C(2) or C(6) of Ar); 111.4 (C(2) or C(6) of Ar); 111.4 ppm (CN); 83.4 (C(4)=*C*); 50.0 (C(2), C(6)); 33.6 (C(3), C(5)); 21.6 (Me). HR-MS: 251.1383 ($C_{16}H_{17}N_3^+$; calc. 251.1422).

2.2.3. *2-[1-(4-fluorphenyl)pyrrolidin-4-ylidene]propanedinitrile* (**5P2**) was synthesized by refluxing **5P1** (193 mg, 1.00 mmol), malononitrile (86 mg, 1.30 mmol), and 89 mg of $AcONH_4$ in 5 ml of toluene for 1.5 h in a *Dean-Stark* apparatus. The usual workup yielded a yellow solid, which was purified by FC (silica gel; petroleum ether 40–60/Et_2O 1:1). Recrystallization from Et_2O/CH_2Cl_2 1:1 yielded **5P2**. Pale-yellow crystals. Yield: 133 mg (0.55 mmol, 55%). M.p. 134–138°. IR ($CHCl_3$): 3020*m*, 2960*m*, 2900*w*, 2810*m*, 2225*s*, 1595*s*, 1505*s*, 825*s*, 810*s*. ^{1}H-NMR (250 MHz, $CDCl_3$): 6.94 (*m*, 4 arom. H); 3.37 (*t*, $J \approx 5.7$, $CH_2(2)$, $CH_2(6)$); 2.86 (*t*, $J \approx 5.6$, $CH_2(3)$, $CH_2(5)$). ^{13}C-NMR (50.3 MHz, APT, $CDCl_3$): 180.0 (C(4)); 157.7 (*d*, *J*(C,F) ≈ 240.7, C(4) of Ar); 145.5 (*d*, *J*(C,F) ≈ 2.5, C(1) of Ar); 118.5 (*d*, *J*(C,F) ≈ 7.7, C(2), C(6) of Ar); 116.0 (*d*, *J*(C,F) ≈ 22.4, C(3), C(5) of Ar); 111.2 (CN); 83.9 (C(4)=*C*); 50.9 (C(2), C(6)); 33.7 (C(3), C(5)). HR-MS: 241.1002 ($C_{14}H_{12}FN_3^+$; calc. 241.1015).

2.2.4. *Methyl 2-Cyano-2-(1-phenylpyrrolidin-4-ylidene)acetate* (**1P3**) was obtained from *Hermant et al.* [21].

2.2.5. *Methyl 2-Cyano-2-[1-(4-methylphenyl)pyrrolidin-4-ylidene]acetate* (**2P3**) was prepared as described for **2P2** by using **2P1** (0.61 g, 3.22 mmol), methyl cyanoacetate (358 mg, 3.61 mmol), 328 mg of $AcONH_4$, and 0.57 ml of AcOH. After the same workup as for **2P2**, the product was purified by FC (silica gel; petroleum ether 40–60/Et_2O 1:) to yield 0.44 g of a yellow solid. Recrystallization from petroleum ether 40–60/Et_2O 1:1 yielded **2P3** as crystals suitable for X-ray analysis. Yield: 0.44 g (1.63 mmol, 51%). M.p. 85.5–86.5°. IR ($CHCl_3$): 3030*m*, 3000*m*, 2950*m*, 2920*m*, 2810*m*, 2220*m*, 1725*s*, 1605*s*, 1508*s*, 808*m*. ^{1}H-NMR (200 MHz, $CDCl_3$): 7.12 (*d*, $J \approx 8.3$, H–C(3), H–C(5) of Ar); 6.87 (*d*, $J \approx 8.6$, H–C(2), H–C(6) of Ar); 3.85 (*s*, MeO); 3.44 (*t*, $J \approx 5.8$, $CH_2(2)$; 3.35 (*m*, $CH_2(6)$); 3.27 (*m*, $CH_2(5)$); 2.90 (*t*, $J \approx 5.7$, $CH_2(3)$); 2.29 (*s*, Me). ^{13}C-NMR (50.3 MHz, APT, $CDCl_3$): 175.9 (C(4)); 162.0 (CO); 147.0 (C(1) of Ar); 129.8 (C(3), C(5) of Ar); 129.6 (C(4) of Ar); 116.3 (C(2), C(6) of Ar); 115.0 (CN); 102.7 (C(4)=*C*); 52.5 (MeO); 50.3 (C(2)); 50.0 (C(6)); 35.2 (C(3)); 30.6 (C(5)); 20.3 (Me). HR-MS: 270.1350 ($C_{16}H_{18}N_2O_2^+$; calc. 270.1368).

REFERENCES

[1] R. Hoffmann, A. Imamura, W.J. Hehre, *J. Am. Chem. Soc.* **1968**, *90*, 1499.

[2] A. W. J. D. Dekkers, J. W. Verhoeven, W. N. Speckamp, *Tetrahedron* **1973**, *29*, 1691.

[3] P. Pasman, J. W. Verhoeven, Th. J. de Boer, *Tetrahedron* **1976**, *32*, 2827; P. Pasman, J. W. Verhoeven, Th. J. de Boer, *Tetrahedron Lett.* **1977**, 207; P. Pasman, J. W. Verhoeven, Th. J. de Boer, *Chem. Phys. Lett.* **1978**, *59*, 381; P. Pasman, N. W. Koper, J. W. Verhoeven, *Recl. Trav. Chim. Pays-Bas* **1982**, *101*, 363; P. Pasman, F. Rob, J. W. Verhoeven, *J. Am. Chem. Soc.* **1982**, *104*, 5127; P. Pasman, G. F. Mes, N. W. Koper, J. W. Verhoeven, *J. Am. Chem. Soc.* **1985**, *107*, 5839; P. Pasman, Ph. D. Thesis, University of Amsterdam, 1980.

[4] G. F. Mes, H. J. van Ramesdonk, J. W. Verhoeven, *Recl. Trav. Chim. Pays-Bas* **1983**, *102*, 55; G. F. Mes, H. J. van Ramesdonk, J. W. Verhoeven, *J. Am. Chem. Soc.* **1984**, *106*, 1335; G. F. Mes, B. de Jong, H. J. van Ramesdonk, J. W. Verhoeven, J. M. Warman, M. P. de Haas, L. E. W. Horsman-van den Dool, *J. Am. Chem. Soc.* **1984**, *106*, 6524; G. F. Mes, Ph. D. Thesis, University of Amsterdam, 1985.

[5] N. S. Hush, M. N. Paddon-Row, E. Cotsaris, H. Oevering, J. W. Verhoeven, M. Heppener, *Chem. Phys. Lett.* **1985**, *117*, 8; J. M. Warman, M. P. de Haas, M. N. Paddon-Row, E. Cotsaris, N. S. Hush, H. Oevering, J. W. Verhoeven, *Nature* **1986**, *320*, 615; J. M. Warman, M. P. de Haas, H. Oevering, J. W. Verhoeven, M. N. Paddon-Row, A. M. Oliver, N. S. Hush, *Chem. Phys. Lett.* **1986**, *128*, 95; J. W. Verhoeven, M. N. Paddon-Row, N. S. Hush, H. Oevering, M. Heppener, *Pure Appl. Chem.* **1986**, *58*, 1285; H. Oevering, M. N. Paddon-Row, M. Heppener, A. M. Oliver, E. Cotsaris, J. W. Verhoeven, N. S. Hush, *J. Am. Chem. Soc.* **1987**, *109*, 3258, H. Oevering, J. W. Verhoeven, M. N. Paddon-Row, J. M. Warman, *Tetrahedron* **1989**, *45*, 4751; H. Oevering, Ph. D. Thesis, University of Amsterdam, 1988.

[6] J. Kroon, A. M. Oliver, M. N. Paddon-Row, J. W. Verhoeven, *Recl. Trav. Chim. Pays-Bas* **1988**, *107*, 509; A. M. Oliver, D. C. Craig, M. N. Paddon-Row, J. Kroon, J. W. Verhoeven, *Chem. Phys. Lett.* **1988**, *150*, 366.

[7] B. Krijnen, Ph. D. Thesis, University of Amsterdam, 1990.

[8] B. Krijnen, H. B. Beverloo, J. W. Verhoeven, C. A. Reiss, K. Goubitz, D. Heijdenrijk, *J. Am. Chem. Soc.* **1989**, *111*, 4433.

[9] D. J. A. De Ridder, K. Goubitz, H. Schenk, B. Krijnen, J. W. Verhoeven, *Helv. Chim. Acta* **2003**, *86*, 812.

[10] D. J. A. De Ridder, K. Goubitz, H. Schenk, B. Krijnen, J. W. Verhoeven, in preparation
[11] G. Jones, in 'Organic Reactions', Eds. R. Adams, A. H. Blatt, V. Boekelheide, T. L. Cairns, A. C. Cope, D. J. Cram, H. O. House; J. Wiley & Sons Inc., New York, 1967, Vol. 15, Chapter 2, p. 204.
[12] R. Hoffmann, *Acc. Chem. Res.* **1971**, *4*, 1; R. Gleiter, *Angew. Chem.* **1974**, *86*, 770; M. N. Paddon-Row, *Acc. Chem. Res.* **1982**, *15*, 245.
[13] W. L. Duax, C. M. Weeks, D. C. Rohrer, *Top. Stereochem.* **1976**, *9*, 271.
[14] D. A. Dougherty, W. D. Hounshell, H. B. Schlegel, R. A. Bell, K. Mislow, *Tetrahedron Lett.* **1976**, 3479; D. A. Dougherty, H. B. Schlegel, K. Mislow, *Tetrahedron* **1978**, *34*, 1441.
[15] N. G. Rondan, M. N. Paddon-Row, P. Caramella, K. N. Houk, *J. Am. Chem. Soc.* **1981**, *103*, 2436; K. N. Houk, N. G. Rondan, F. K. Brown, W. L. Jorgensen, J. D. Madura, D. C. Spellmeyer, *J. Am. Chem. Soc.* **1983**, *105*, 5980.
[16] G. A. Jeffrey, K. N. Houk, M. N. Paddon-Row, N. G. Rondan, J. Mitra, *J. Am. Chem. Soc.* **1985**, *107*, 321.
[17] R. de Gelder, R. A. G. de Graaff, H. Schenk, *Acta Crystallogr., Sect. A* **1993**, *49*, 287.
[18] 'XTAL3.7 System', Eds. S. R. Hall, D. J. du Boulay, R. Olthof-Hazekamp, University of Western Australia, Lamb, Perth, Australia, 2000.
[19] W. H. Zachariasen, *Acta Crystallogr.* **1967**, *23*, 558.
[20] A. L. Spek, *Acta Crystallogr., Sect. A* **1990**, *46*, C-34.
[21] R. M. Hermant, N. A. C. Bakker, T. Scherer, B. Krijnen, J. W. Verhoeven, *J. Am. Chem. Soc.* **1990**, *112*, 1214.

Received September 24, 2002